*Ocean Systems Engineering, Vol. 2, No. 4 (2012) 297-314*
DOI: http://dx.doi.org/10.12989/ose.2012.2.4.297


# Wave energy converter by using relative heave motion between buoy and inner dynamic system

I.H. Cho*[1], M.H. Kim[2] and H.M. Kweon[3]

[1]*Department of Ocean System Engineering, Jeju National University, Jeju 690-756, Korea*
[2]*Department of Civil Engineering, Texas A&M University, College Station, Texas, 77843, USA*
[3]*Department of Civil Engineering, Kyongju University, Kyongju, Korea*

*(Received December 3, 2012, Revised December 9, 2012,Accepted December 14, 2012)*

**Abstract.** Power-take-off through inner dynamic system inside a floating buoy is suggested. The power take-off system is characterized by mass, stiffness, and damping and generates power through the relative heave motion between the buoy and inner mass (magnet or amateur). A systematic hydrodynamic theory is developed for the suggested WEC and the developed theory is illustrated by a case study. A vertical truncated cylinder is selected as a buoy and the optimal condition of the inner dynamic system for maximum PTO (power take off) through double resonance for the given wave condition is systematically investigated. Through the case study, it is seen that the maximum power can actually be obtained at the optimal spring and damper condition, as predicted by the developed WEC theory. However, the band-width of high performance region is not necessarily the greatest at the optimal (maximum-power-take-off) condition, so it has to be taken into consideration in the actual design of the WEC.

**Keywords:** heave motion; linear electric generator; power absorption; matched eigenfunction expansion method; double resonance; power take off; high performance band-width

## 1. Introduction

Ocean waves hold enormous energy. The harvestable wave power is estimated to be as much as 10 TW, about two thirds of total worldwide energy demand of 15 TW in 2008. Unfortunately however, ocean wave energy is highly underutilized until recently. The primary limiting factors are the efficiency of PTO system, survivability in harsh storm conditions, and high installation/maintenance cost. Numerous ideas have been proposed for harvesting wave energy (e.g., McCormick 2007, Grilli *et al.* 2007, Gato and Falcão 1988, Koo and Kim 2010). This paper proposes a new point absorber that enhances the effectiveness of PTO by taking advantage of properly tuned relative motions between floating buoy and inner dynamic system.

There have been many researches regarding the performance of a point absorber as WEC since 1970s. Mostly, they take advantage of large resonant motions of a floating buoy and the electricity is generated by hydraulic PTO system or linear generator system. As for the latter, a floating buoy is to move with respect to fixed (or minimal heave) core structure and generates electricity by using the relative motion. In this case, either the buoy or core structure has to function as a magnet or

*Corresponding author, Professor, E-mail: cho0904@jejunu.ac.kr

amateur (coil) in a wet condition. In the present study, we introduce an inner mass (or magnet) inside a buoy and utilize the relative heave motion between the buoy and the inner mass. This can be operated inside the buoy with dry condition, so the overall system should be much safer, simpler, and more cost-effective. Moreover, the efficiency can further be enhanced by using double resonance between the buoy and inner mass. In the preliminary design of such WECs, the PTO system can be simplified as an equivalent linear spring-damper system. In this paper, a hydrodynamic theory regarding how to maximize its efficiency through double resonance is developed.

In the present study, we selected a vertical truncated cylinder as a buoy and tried to find the optimal condition of the inner dynamic system for maximum PTO. The wave interactions with a floating truncated vertical cylinder have been studied by many researchers (e.g., Miles and Gilbert 1968, Garret 1971, Tung 1979, McIver and Evans 1984). In the present paper, the diffraction/radiation of the floating truncated vertical cylinder is solved by using the eigenfunction expansion method in view of expanding the method to multiple cylinders to form a farm. The general linear hydrodynamic theory for a single point absorber with a simple PTO was developed by, for example, Evans (1976), Newman (1975), French and Bracewell (1985), Kim and Choi (1983). The PTO theory by using the arrays of such WECs is also given in Budal and Falnes (1975), Srokosz and Evans (1979), Kim and Choi (1983). The actual PTO system by linear generator with a floating buoy and core structure has been investigated by Elwood *et al.* (2007). A similar inner PTO system by using resonant relative motions was also introduced in Beatty *et al.* (2008).

The conceptual design of the WEC under consideration is shown at Fig. 1. It consists of a vertical-cylinder buoy and an exterior torus frame with 3 legs for positioning and minimizing pitch motion. The legs are connected to the seabed through vertical tendons (vertical mooring). The top tensions of the tendons are provided by the net buoyancy of the torus-subbuoy-with-3-leg system. When the buoy contacts the frame, the possible friction in heave direction is avoided by using suitable rollers imbedded in the frame. Otherwise, the heave motion of the buoy is independent and not influenced by the subbuoy-leg mooring system. Since the vertical motion of the subbuoy-leg system is restricted by tendons, the relative motion between the subbuoy and cylindrical buoy is

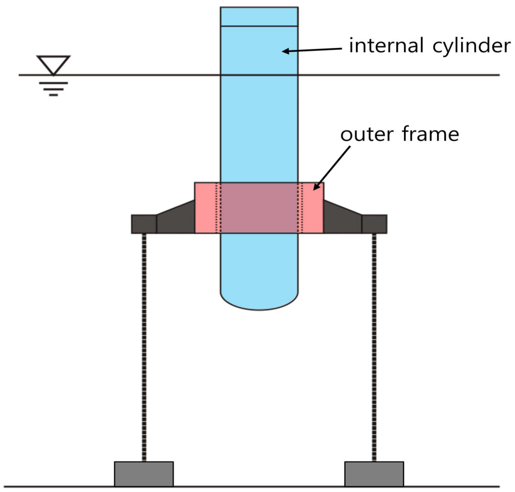


Fig. 1. Conceptual design of wave energy converter

also large, which can be utilized for power generation through a wet linear generator between them. This way, electricity can be generated from both inside and outside of the cylindrical buoy to maximize its efficiency. In the present study, however, it is assumed that the subbuoy-leg system is used only for station-keeping purpose. Since there are no mooring lines directly connected to the cylindrical buoy, it can easily escape the worst storm after sinking the subbuoy to the seafloor by water ballast. After storm, the reverse steps can be applied to restore to the original set up.

With this kind of arrangement, the pitch motion of the buoy, which may hamper the effectiveness of the heave-relative-motion-based PTO through coupling, can be reduced to minimal values. With the vertical mooring system, surge motions may be allowed but the surge mode is not coupled with the heave mode, so it does not affect the performance of the proposed power-generation system. In this regard, surge and pitch motions of the cylinder buoy are not considered in the following power-generation-efficiency analysis. It is also assumed that the disturbance of the incident and diffracted/radiated wave fields by the outer slender frame and legs is negligible. This assumption makes sense because it is relatively slender and deeply submerged. In this paper, the hydrodynamic performance of the proposed WEC in various design parameters and irregular-wave conditions is presented. The general strategy to achieve high performance is suggested through numerical examples. The present theory and methodology can straightforwardly be extended to arrays of such point absorbers, which will be the subject of forthcoming study.

## 2. Mathematical formulation

We consider the diffraction and radiation of waves by a spar buoy of cylindrical shape, with radius $a$ and draft $d$, floating in water of uniform depth $h$. The definition sketch for a cylindrical spar buoy is shown in Fig. 2. The cylindrical coordinates are chosen with the origin at the center of buoy on free surface and z-axis pointing vertically upward. Under the assumption of linear potential theory, the fluid velocity can be described by the gradient of velocity potential $\Phi(r, \theta, z, t)$ with linear boundary conditions. Assuming harmonic motion of frequency $\omega$, the velocity potential can

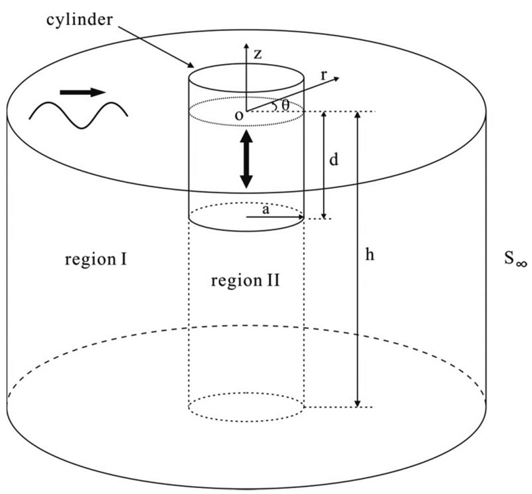


Fig. 2. Definition sketch of a floating spar buoy

be written as $\Phi(r, \theta, z, t) = Re[\phi(r, \theta, z, t)e^{-i\omega t}]$. The total velocity potential can be expressed by the sum of incident wave potential, diffraction potential, and radiation potential.

$$\phi(r, \theta, z) = -\frac{ig}{\omega}A\sum_{i=0}^{\infty}[\phi_I^l(r,z)+\phi_D^l(r,z)]\cos l\theta - i\omega z_o\phi_R(r,z) \tag{1}$$

where $A$ is the incident wave amplitude and $z_o$ is the heave amplitude of a spar buoy. In the present study, only a heave motion is considered although including other degrees of freedom is straightforward. Since the body is axisymmetric, heave mode is independent of other modes. The radiation problem for heave is a function of $r$ and $z$.

### 2.1 Diffraction problem

To apply the matched eigenfunction expansion method (MEEM), the fluid is divided into region (I) and region (II). Region (I) is defined by $r > a$, $-h < z < 0$, and region (II) by $r < a$, $-h < z < -d$. The velocity potential($\phi_S^{l(1)}$) in region (I), satisfying Laplace's equation in fluid, the linear free-surface condition, bottom condition, and radiation condition, can be expressed by the sum of incident and diffraction potentials.

$$\phi_S^{l(1)} = \beta_l J_l(k_1 r)\frac{\cosh k_1(z+h)}{\cosh k_1 h} + \sum_{n=0}^{\infty} B_{ln}\frac{K_l(k_{1n}r)}{K_l(k_{1n}a)}\Psi_{1n}(z) \tag{2}$$

where $\beta_l$ is defined by $\beta_l = 1$ if $l = 0$, and $\beta_l = 2(i)^l$ if $l \geq 1$. $n = 0$ denotes propagating mode while $n \geq 1$ represent evanescent modes. $J_l$ and $K_l$ are Bessel and modified Bessel functions.

The eigenvalues ($k_{10} = -ik_1$, $k_{1n}$, $n = 1, 2, ...$) in region (I) satisfy the dispersion relation $k_{1n} \tan k_{1n}h = -\omega^2/g$ and the normalized eigenfnctions can be written as

$$\begin{aligned}\Psi_{1n}(z) &= N_{1n}^{-1}\cos k_{1n}(z+h),\ n = 0, 1, 2, ... \\ N_{1n}^2 &= \frac{1}{2}\left(1+\frac{\sin 2k_{1n}h}{2k_{1n}h}\right)\end{aligned} \tag{3}$$

The eigenfunctions $\Psi_{1n}$ satisfy following orthogonal relation.

$$\frac{1}{h}\int_{-h}^{0}\Psi_{1m}(z)\Psi_{1n}(z)dz = \delta_{mn} \tag{4}$$

where $\delta_{mn}$ is the Kronecker delta function defined by $\delta_{mn} = 1$ if $m = n$, and $\delta_{mn} = 0$ if $m \neq n$.

he velocity potential in region (II), satisfying Laplace's equation and bottom condition, can be written as

$$\phi_S^{l(2)} = A_{l0}\left(\frac{r}{a}\right)^l + 2\sum_{n=1}^{\infty} A_{ln}\frac{I_l(\lambda_n r)}{I_l(\lambda_n a)}\cos\lambda_n(z+h) \tag{5}$$

where $\lambda_n = n\pi/c$, $(n = 0, 1, 2, ...)$, $c = h-d$.

The velocity potential in each region must be matched at $r = a$ by the matching boundary condition i.e., $\phi$ and $\partial\phi/\partial r$ are continuous across $r = a$. If the matching condition for $\phi$ is imposed and the resulting equation is multiplied by the set of eigenfunctions $\{cos\lambda_m(z+h),\ m=0,1,2,...\}$ and integrated over $(-h,\ -d)$, we obtain

$$g_{lm}+A_{lm} = \sum_{n=0}^{\infty} B_{ln}\, G_{mn},\ m,l = 0,1,2,... \tag{6}$$

where

$$g_{lm} = -\frac{\beta_l J_l(k_1 a)}{c}\int_{-h}^{-d}\frac{cosh_1(z+h)}{cosh_1 h}cos\lambda_m(z+h)dz$$

$$G_m = \frac{1}{c}\int_{-h}^{-d} cos\lambda_m(z+h)\,\Psi_{1n}(z)dz = \frac{(-1)^m k_{1n}\sin k_{1n}c}{N_{1n}c(k_{1n}^2-\lambda_m^2)}$$

Continuity of $\partial\phi/\partial r$ at $r=a$ gives

$$\frac{1}{h}\left[\beta_l k_1 h J_l'(k_1 a)\frac{coshk_1(z+h)}{coshk_1 h}+\sum_{n=0}^{\infty} B_{ln}\, q_{ln}\ \Psi_{1n}(z)\right] = \begin{cases} 0, & -d<z<0 \\ \dfrac{2}{c}\displaystyle\sum_{n=0}^{\infty} A_{ln}\, p_{ln}\ cos\lambda_n(z+h), & -h<z<-d \end{cases} \tag{7}$$

where

$$p_{ln} = \begin{cases} \dfrac{cl}{2a}, & n = 0 \\ \dfrac{\lambda_n c I_l'(\lambda_n a)}{I_l(\lambda_n a)}, & n \geq 1 \end{cases}$$

$$q_{ln} = \frac{k_{1n}hK_l'(k_{1n}a)}{K_l(k_{1n}a)}$$

Eq. (7) can then be multiplied by each of the eigenfunction $\{\Psi_{1m}(z), m=0,1,2,...\}$ and integrated over $(-h,\ 0)$ , which results in

$$B_{lm}q_{lm} = -\frac{\beta_l k_1 h J_l'(k_1 a)N_{10}}{coshk_1 h}\delta_{m0}+2\sum_{n=0}^{\infty} A_{ln}\, p_{ln}\, G_{nm},\ \ m,l=0,1,2,... \tag{8}$$

If Eqs. (6) and (8) are combined by eliminating the unknown coefficients $A_{lm}$, we obtain the simultaneous algebraic equations for the unknown constants $B_{lm}$

$$B_{lm}+\sum_{n=0}^{\infty}\frac{F_{lmn}}{q_{lm}}B_{ln} = \frac{X_{lm}}{q_{lm}},\quad m,l = 0,1,2,... \tag{9}$$

where

$$F_{lmn} = -2\sum_{k=0}^{\infty} p_{lk}G_{kn}G_{km}$$

$$X_{lm} = -\frac{\beta_l k_1 h J_l'(k_1 a) N_{10}}{coshk_1 h}\delta_{m0} - 2\sum_{k=0}^{\infty} p_{lk} q_{lk} G_{km}$$

The above matrix equations can be solved by truncating $m$ and $n$ to $N$ for the given integer $l$ = 0, 1, 2,...$M$. The unknown coefficients $A_{lm}$ can be readily obtained from Eq. (6).

From the solutions of velocity potential, the vertical wave exciting forces on a spar buoy can be found by integrating the pressure over its bottom surface.

$$F_D = AXe^{-i\omega t}, \text{with } X = 2\pi\rho a\int_0^a r\phi_S^{0(2)}(r,-d)dr. \tag{10}$$

### 2.2 Radiation problem

The radiation problem by the vertical oscillation of a spar buoy can be solved in similar way as the diffraction problem. The velocity potential in region (I) can be expressed by

$$\phi_R^{(1)} = \sum_{n=0}^{\infty} B_n^* \frac{K_0(k_{1n} r)}{K_0(k_{1n} a)}\psi_{1n}(z) \tag{11}$$

The velocity potential in region (II) can be written as the sum of a particular solution and a homogeneous solution.

$$\phi_R^{(2)} = \phi_P^{(2)} + \sum_{n=0}^{\infty} \varepsilon_n A_n^* \frac{I_0(\lambda_n r)}{I_0(\lambda_n a)} cos\lambda_n(z+h) \tag{12}$$

where $\varepsilon_n = 1$ if $n$ = 0, and $\varepsilon_n = 2$ if $n \geq 1$. The particular solution satisfying the inhomogeneous body-boundary condition ($\partial\phi_P^{(2)}/\partial z = 1$ at $z = -d$) is given by

$$\phi_P^{(2)} = \frac{1}{2c}\left((z+h)^2 - \frac{r^2}{2}\right) \tag{13}$$

From the matching condition that $\phi$ and $\partial\phi/\partial r$ must be continuous across $r = a$, we obtain the following algebraic equations.

$$B_m^* + \sum_{n=0}^{\infty} \frac{F_{0mn}}{q_{0m}} B_n^* = \frac{X_m^*}{q_{0m}}, \qquad m = 0, 1, 2, ... \tag{14}$$

where

$$X_m^* = -\frac{a}{2}G_{0m} - 2\sum_{k=0}^{\infty} p_{0k}\, q_{0k} G_{km}$$

The remaining unknown coefficients $A_m^*$ in region (II) can then be determined from

$$A_m^* = \sum_{k=0}^{\infty} B_k^* G_{mk} - \frac{1}{c}\int_{-h}^{-d} \phi_P^{(2)}(a,z) cos\lambda_m(z+h)dz, \quad m \geq 0 \tag{15}$$

The hydrodynamic forces by the heave oscillation of a spar buoy are found by integrating the pressure over bottom surface of cylinder.

$$F_R = 2\pi\rho\omega^2 z_0 \int_0^a r\phi_R^{(2)}(r,-d)dre^{-i\omega t} = (\omega^2\mu + i\omega v)z_0 e^{-i\omega t} \tag{16}$$

where $\mu$ and $v$ are added mass and radiation damping, respectively.

### 2.3 Equation of motion

The equation of heave motion of a spar buoy is given by

$$(m_1 + \mu)\ddot{z} + B\dot{z} + \rho g S z = F_D \tag{17}$$

where the upper dots denote time derivatives, $m_1(= \rho Sd)$ is the buoy mass together with the equipment attached to it, and $S(= \pi a^2)$ is the water-plane area. $B(= b + v)$ is total-damping coefficients with $b$ = viscous damping coefficient and $v$ = radiation damping coefficient. The damping factor $\kappa$ and undamped natural frequency $\omega_o$ are defined as $B = \dfrac{2\kappa\rho g S}{\omega_o}$ and $\omega_o = \sqrt{\dfrac{\rho g S}{m_1 + \mu}}$ with $\mu$ being the added mass. The damping factor $\kappa$ including viscous effects can be determined from a free-decay test in still water.

Fig. 3 shows the heave free-decay test results of the present cylindrical buoy with a initial displacement 0.1m. The scale ratio of 1/10 ($b$ = 0.5 m, $2a$ = 0.1 m) was used for the experiment (Rho *et al.* 2002). Assuming linear dynamic system, the non-dimensional damping factor $\kappa$ can be estimated from two successive peaks as follows

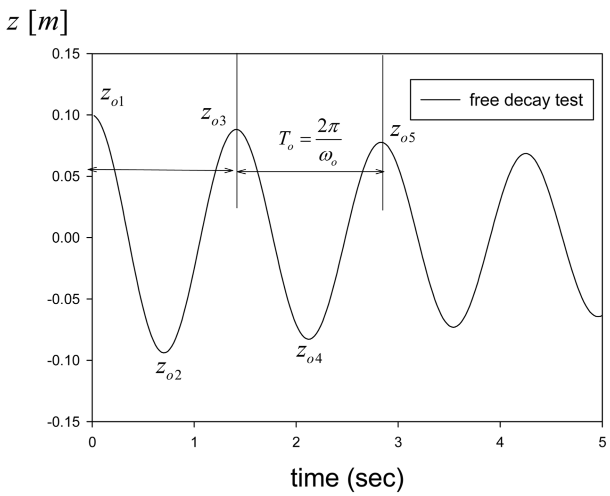


Fig. 3. Free-decay test results obtained from the experiments of Rho *et al.* (2002)

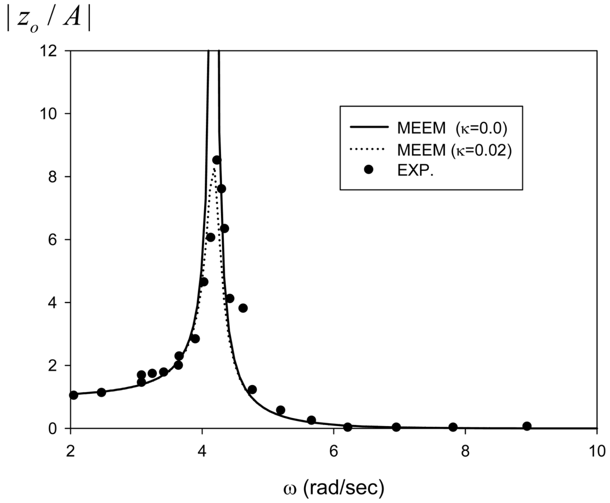


Fig. 4. Comparison of heave RAO with the experimental measurements (Rho *et al.* 2002)

$$\kappa = \frac{1}{2\pi} ln \left\{ \frac{z_{o1} - z_{o2}}{z_{o3} - z_{o4}} \right\} \approx 0.02 \tag{18}$$

Fig. 4 shows the heave RAO (Response Amplitude Operator) curve obtained from the measurement (Rho *et al.* 2002) and calculation with $\kappa = 0.02$. The solid line denotes the potential results ignoring effects ($\kappa = 0.02$), the dotted line is the computation with $\kappa = 0.02$, and the circles represent measured data. The numerical result with experimentally fitted damping factor shows a good fit against the experimental results. Afterward, the non-dimensional damping factor $\kappa$ is fixed at 0.02.

### *2.4 Dynamics of LEG(linear electric generator)*

The LEG is inside the buoy and for power take-off. It consists of mass and linear damper/spring. It is assumed that it can represent either a magnet movement or simplified model of hydraulic system. The motion of a spar buoy induces the motion of the LEG system, also the LEG dynamics affect the motion of a spar buoy. The applied spring stiffness is $k$, damping $c$, and magnet mass $m_2$. It is also assumed that the mass is constrained to oscillate only in the vertical direction. We consider the two-body (spar buoy and magnet) system represented in Fig. 5. Let $z$ and $y$ be the coordinates for the heave motion of buoy and magnet. The equations of motion for the two-body system can be written by

$$(m_1 + \mu)\ddot{z} + m_2\ddot{y} + B\dot{z} + \rho g S z = F_D$$
$$m_2\ddot{y} + c(\dot{y} - z) + k(y - z) = 0 \tag{19}$$

where the damping coefficient of LEG system $c$ represents a controllable parameter related to electro-magnetic interactions, as a function of the magnet strength and coil circuit characteristics.

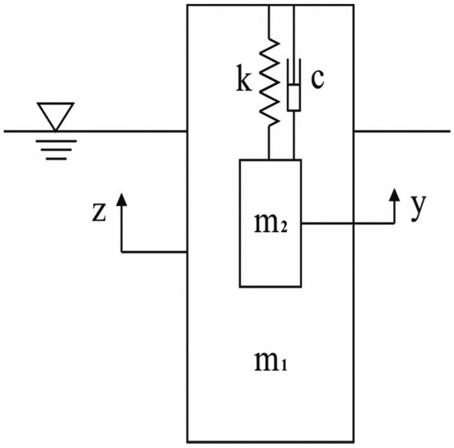


Fig. 5. Linear electric generator (LEG)

The mechanical power extracted from the relative velocity $\dot{x}(=\dot{y}-\dot{z})$ between the spar buoy and magnet is $P(t)=c\dot{x}^2$. The undamped natural frequency of LEG system is $\omega_G=\sqrt{k/m_2}$.

The whole system is linear, we may write $z=z_oe^{-i\omega t}$, $y=y_oe^{-i\omega t}$, $x=x_oe^{-i\omega t}$ under the assumption of monochromatic incident waves of frequency $\omega$. From Eq. (19), we obtain

$$[-\omega^2(M+\mu)-i\omega B+\rho gS]z_o-\omega^2m_2x_o=AX$$
$$-\omega^2m_2z_o+(-\omega^2m_2-i\omega c+k)x_o=0 \tag{20}$$

where $M(=m_1+m_2)$ is a total mass. After dividing Eq. (20) by $m_2\omega^2$ and rearranging, Eq. (20) can be reduced to

$$(U-iV)z_o-x_o=AQ$$
$$-z_o+(S-iT)x_o=0 \tag{21}$$

which are readily solved to give the heave amplitude of a spar buoy and the relative heave amplitude between the magnet and buoy normalized by incident wave amplitude $A$.

$$\frac{x_o}{A}=\frac{Q}{(U-iV)(S-iT)-1}$$
$$\frac{z_o}{A}=\frac{(S-iV)Q}{(U-iV)(S-iT)-1} \tag{22}$$

where

$$U=\frac{\rho gS-\omega^2(M+\mu)}{m_2\omega^2},\quad V=\frac{B}{m_2\omega},\quad Q=\frac{X}{m_2\omega^2}$$

$$S=\frac{k}{m_2\omega^2}-1,\ T=\frac{c}{m_2\omega}$$

The time-averaged power per unit wave amplitude is given by

$$\frac{\bar{P}}{A^2} = \frac{1}{2}c\omega^2\left|\frac{x_o}{A}\right|^2 = \frac{1}{2}\frac{c\omega^2|Q|^2}{|(U-iV)(S-iT)-1|^2} = \frac{1}{2}\frac{m_2\omega^3T|Q|^2}{(US-VT-1)^2(VS+UT)^2} \tag{23a}$$

To maximize $\bar{P}/A^2$ with respect to the two control parameters $S$ and $T$, we differentiate Eq. (22) with respect to $S$ and $T$. Then, we obtain the conditions $S_{opt} = U/W^2$, $T_{opt} = V/W^2$ with $W^2 = U^2 + V^2$ for optimal power capture. The maximum power take-off condition can be rewritten as

$$S_{opt} = \frac{k-m_2\omega^2}{m_2\omega^2} = \frac{m_2\omega^2(\rho gS-(M+\mu)\omega^2)}{(\rho gS-(M+\mu)\omega^2)^2+(B\omega)^2}$$

$$T_{opt} = \frac{c}{m_2\omega} = \frac{m_2B\omega^3}{(\rho gS-(M+\mu)\omega^2)^2+(B\omega)^2} \tag{23b}$$

By using the above two equations, the optimal stiffness and damping of the inner dynamic system can be determined from the given floater particulars and incident wave frequency.

If $\omega$ is at the buoy heave resonance $(\rho gS-(M+\mu)\omega^2) = 0$, or $S_{opt} = 0$, and $k_{opt} = m_2\omega^2$. Under the same resonance condition, $T_{opt} = \frac{c}{m_2\omega} = \frac{m_2\omega}{B}$. Considering $B = 2\kappa(M+\mu)\omega$, we obtain $c_{opt}/m_2\omega \approx 0.5$ for $m_2/M = 0.02$, $\kappa = 0.02$. If both conditions are satisfied, the corresponding power take-off becomes maximum for the present set up. In irregular waves, it is impossible to satisfy the optimal condition for all component waves simultaneously. Therefore, a good choice is satisfying the condition for the peak frequency of the incident wave spectrum.

Substituting the optimal conditions into Eq. (23(a)) gives the ideal power

$$\frac{\bar{P}_{\max}}{A^2} = \frac{1}{8}\frac{m_2\omega^3|Q|^2}{V} = \frac{|X|^2}{8B} \tag{24}$$

This is a well-known result derived by Evans (1976) for the maximum capture of wave energy by using a single mode of heave motion.

For irregular waves, the heave-motion spectrum, the relative-motion spectrum, and the square root power spectrum are computed from

$$S_z(\omega) = \left|\frac{z_o}{A}(\omega)\right|^2 \cdot S_\varsigma(\omega)$$

$$S_x(\omega) = \left|\frac{x_o}{A}(\omega)\right|^2 \cdot S_\varsigma(\omega)$$

$$S_{\sqrt{P}}(\omega) = \frac{\bar{P}(\omega)}{A^2} \cdot S_\varsigma(\omega) \tag{25}$$

As the incident wave spectrum $S_\varsigma(\omega)$, the TMA spectrum (Bouws *et al.* 1985) is used for giving the possibility of developing a finite water depth form

$$S_\varsigma(\omega) = S_J(\omega) \cdot F(\omega_*) \tag{26}$$

where $S_J(\omega)$ is the JONSWAP spectrum suggested by Goda (1988) and $F(\omega_*)$ is given by

$$S_J(\omega) = \beta \frac{H_{1/3}^2 \omega_P^4}{\omega^5} exp\left[-1.25\left(\frac{\omega}{\omega_P}\right)^{-4}\right] \gamma^{exp\left[-\frac{(\omega-\omega_P)^2}{2\sigma^2\omega_P^2}\right]}$$

$$\text{with } \beta = \frac{0.0624}{0.23 + 0.0336\gamma - 0.185(1.9+\gamma)}(1.094 - 0.01915\ln\gamma) \tag{27}$$

$$F(\omega_*) = f^{-2}\left[1 + \frac{2\omega_* f}{\sinh(2\omega_* f)}\right]^{-1}$$

where $1 = f\,tanh(\omega_*^2 f)$ and $\omega_*^2 = \dfrac{\omega^2 h}{g}$, $H_{1/3}$ is significant wave height and $\omega_P\left(= \dfrac{2\pi}{T_P}\right)$ is peak circular frequency. $\gamma = 3.3$, $\sigma = 0.07$ for $\omega < \omega_P$ and $\sigma = 0.09$ for $\omega \geq \omega_P$.

The significant buoy-heave amplitude, significant relative-motion amplitude, and significant amplitude of square root power in irregular waves can be obtained

$$z_{a1/3} = 2\sqrt{\int_0^\infty S_z(\omega)d\omega}$$
$$x_{a1/3} = 2\sqrt{\int_0^\infty S_x(\omega)d\omega} \tag{28}$$
$$\sqrt{P}_{1/3} = 2\sqrt{\int_0^\infty S_{\sqrt{P}}(\omega)d\omega}$$

## 3. Numerical results and discussions

As a numerical model, we adopt a spar buoy of diameter 1.0 m, and draft 5.0 m in water of depth 30 m, as shown in Fig. 2. The heave natural frequency of a spar buoy can be predicted by $\omega_o \approx \sqrt{g/(1+\alpha)d} = 1.36$ rad/sec, where added mass coefficient $\alpha = \mu/m_1 = 0.06$. If the heave added mass is not counted, $\omega_o = 1.39$ rad/sec. The magnet mass to total mass ratio $m_2/M$ is fixed at 0.02. As key design parameters, the non-dimensional spring stiffness $k/m_2\omega_o^2$ and damping $c/m_2\omega_o$ of LEG system are adopted. If $k/m_2\omega_o^2 = 1.0$, it means double resonance. This is one of the two conditions for maximum power take-off. Therefore, for the maximum relative motion, the natural

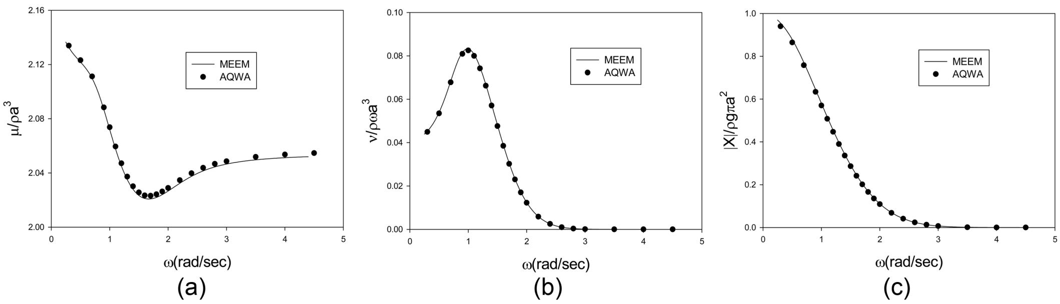


Fig. 6. (a) Comparison of non-dimensional added mass, (b) radiation damping, and (c) exciting force from present MEEM solutions with ANSYS AQWA numerical results($h$ = 30 $m$, $d$ = 5.0 $m$, $2a$ = 1.0 $m$)

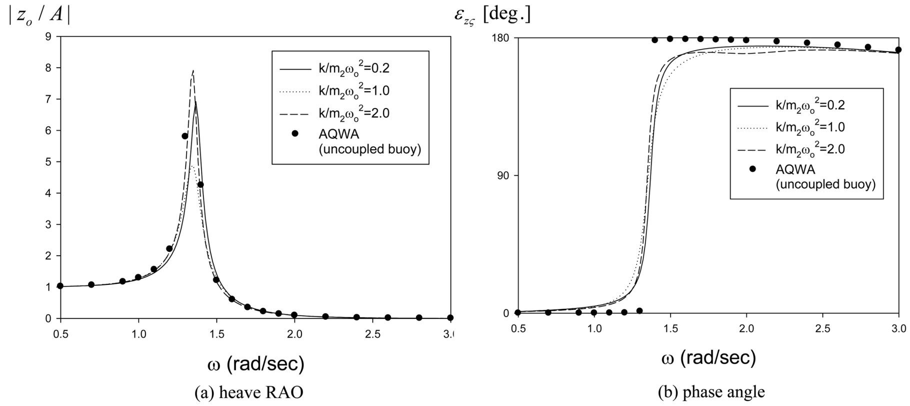


Fig. 7. Heave motion (RAO, phase angle) of a spar buoy as a function of non-dimensional spring stiffness and wave frequency for $c/m_2\omega_o = 0.5$

period of LEG ($\omega_G = \sqrt{k/m_2}$) needs to coincide with hull natural frequency $\omega_o$.

First, the analytic solutions developed in Sec. 2 are compared with the BEM-based numerical solutions (commercial panel program AQWA). Fig. 6 shows the non-dimensional added mass, radiation damping, and wave exciting force vary for heave as function of wave frequency $\omega$. The solid lines are the analytic solutions calculated with the number of eigenfunctions $M$ = 20, $N$ = 60 and the symbols are for ANSYS AQWA solutions with 2881 total elements on body surface. The two solutions are in good agreement.

Fig. 7 shows the heave RAOs of the buoy and their phases for three different spring coefficients and the results are also compared with the RAO by AQWA without considering the coupling with inner dynamic system. For these results, the dimensionless inner-system damping is fixed at optimal value $c/m_2\omega_o = 0.5$. Under this condition, the optimal condition can be achieved only at $\omega = \omega_o$. It is seen that the buoy heave amplitude is appreciably affected by the coupling with inner dynamic system only near the resonance region. The buoy resonant motion becomes minimal at the optimal condition $k/m_2\omega_o^2 = 1.0$ since the inner dynamic system functions as a vibration absorber at that condition, which is practically beneficial. In such a narrow resonance region, the phase of buoy heave motion relative to the incident wave is suddenly changed from 0 to 180 degrees. In Fig. 8, the relative heave displacements and phases between the buoy and inner-mass are plotted for the same conditions as in Fig. 7. High stiffness slightly improves performance in high frequency region

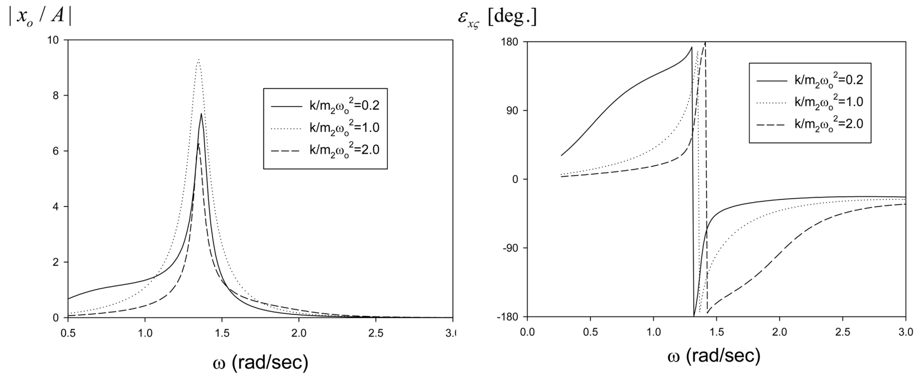


(a) relative heave RAO (b) phase angle

Fig. 8. Relative heave motion (RAO, phase angle) of a magnet mass with respect to a spar buoy as a function of non-dimensional spring stiffness and wave frequency for $c/m_2\omega_o = 0.5$

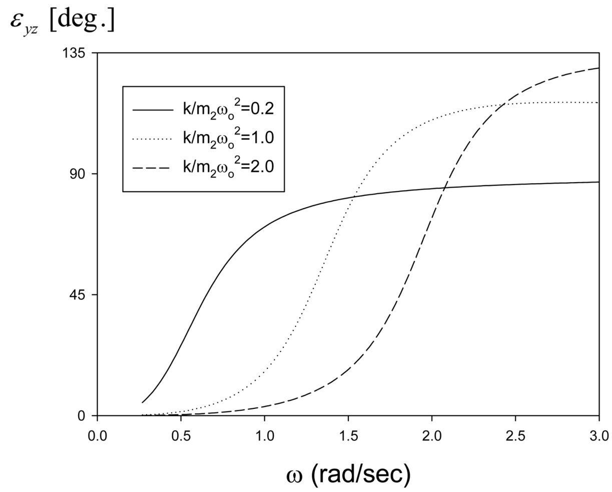


Fig. 9. Phase angle shift between a magnet mass ($y$) and a spar buoy ($z$) as a function of non-dimensional spring stiffness and wave frequency for $c/m_2\omega_o = 0.5$

but worsens performance in low frequency region. We can see the largest relative displacement at the optimal condition $k/m_2\omega_o^2 = 1.0$. The band width of high performance is also appreciably increased at the optimal condition, which is practically important. At the resonance condition, the phase difference between the relative displacement and incident wave is about 180 degrees.

Fig. 9 shows the phase-angle shift between the buoy and inner mass as function of wave frequency. As was pointed out by Omholt (1978), the phase of buoy motion is about 90-degree ahead of the phase of magnet motion near the resonance region.

Fig. 10 shows the buoy heave amplitude and buoy-magnet relative heave amplitude as functions of wave frequencies with varying magnet damping coefficients for the fixed optimal spring parameter $k/m_2\omega_o^2 = 1.0$. The power-take-off is proportional to damping but larger damping decreases the relative motion. Therefore, it is not that straightforward to decide which is the most desirable damping by just looking at displacement results like Fig. 10.

Fig. 11 shows the phase-angle between the buoy and inner mass as function of wave frequency

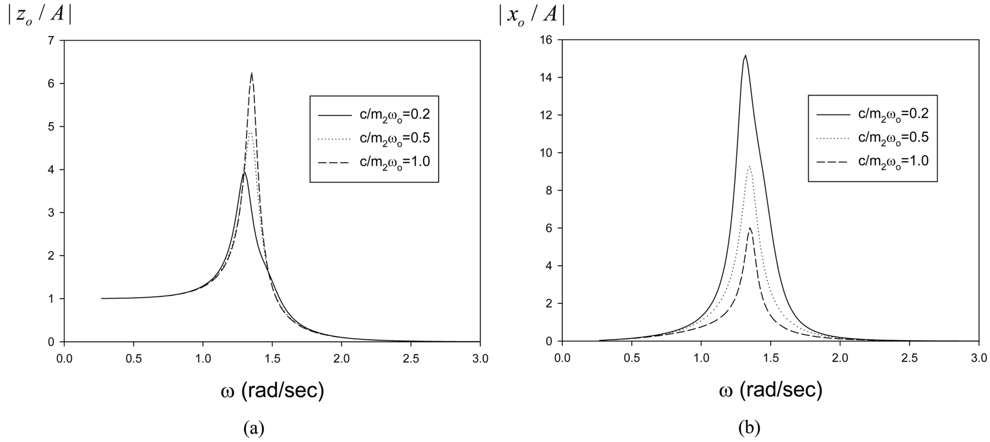


Fig. 10. (a) Heave RAO and (b) relative heave RAO as a function of non-dimensional LEG system damping and wave frequency for $k/m_2\omega_o^2 = 1.0$

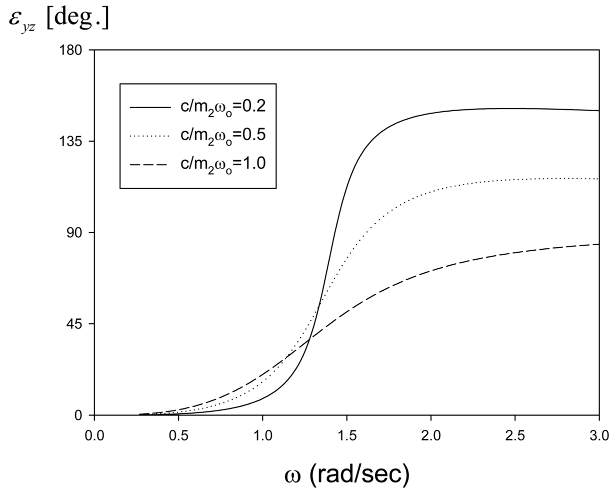


Fig. 11. Phase angle shift between a magnet mass ($y$) and a spar buoy ($z$) as a function of non-dimensional LEG system damping and wave frequency for $k/m_2\omega_o^2 = 1.0$

for the fixed spring stiffness and various damping coefficients. We can see that larger phase shifts occur when smaller damping coefficients are used, which results in larger relative displacements. When compared to Evan's theoretical curve, Fig. 12 shows that the maximum wave power can actually be taken at the optimal damping coefficient $c/m_2\omega_o = 0.5$. However, the case $c/m_2\omega_o = 0.2$ looks even better by appreciably increasing the high-performance band-width although the maximum possible power is not reached. On the other hand, the higher damping values reduce both the peak amplitude and the band-width. From this point on, let us consider the body responses and available hydrodynamic power in irregular waves, represented by the wave amplitude spectrum of Fig. 13.

The corresponding relative motion spectra and power-take-off spectra for various spring parameters are given in Fig. 14 for the fixed damping parameter. It is seen that the maximum

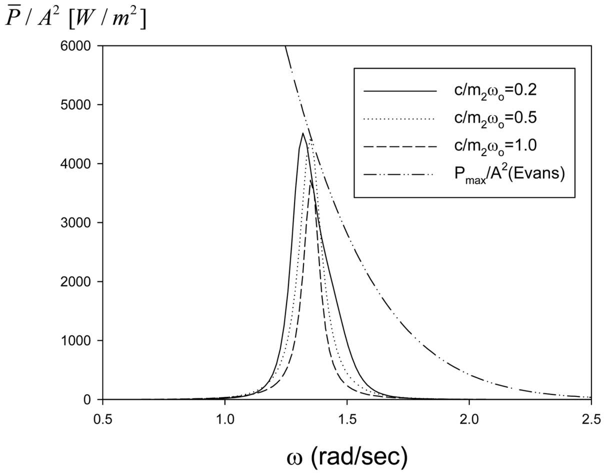


Fig. 12. Time-averaged power ($\overline{P}/A^2$) as a function of non-dimensional LEG system damping and wave frequency for $k/m_2\omega_o^2 = 1.0$

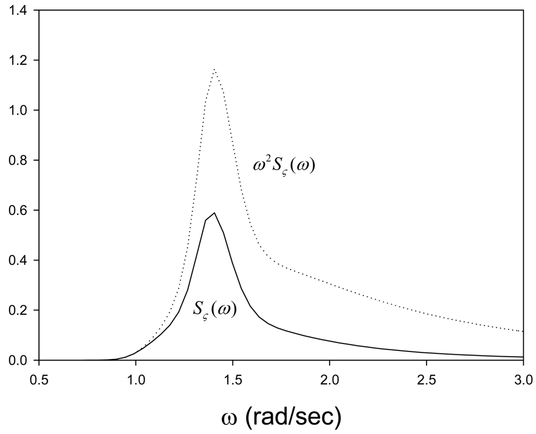


Fig. 13. Wave and velocity spectrum for $H_{1/3} = 2.0\ m$, $\omega_P = 1.39$ red/sec, $\gamma = 3.3$

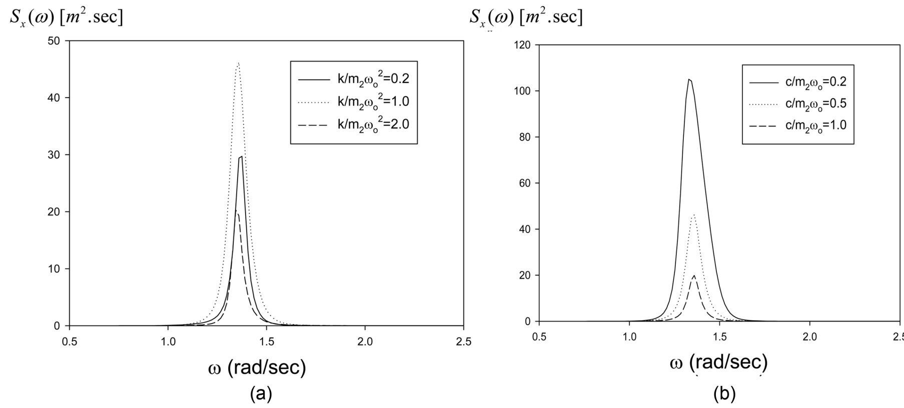


Fig. 14. (a) Relative motion spectrum and (b) square root power spectrum as a function of non-dimensional spring stiffness and wave frequency for $H_{1/3} = 2.0\ m$, $\omega_P = 1.39$ red/sec, $c/m_2\omega_o = 0.5$

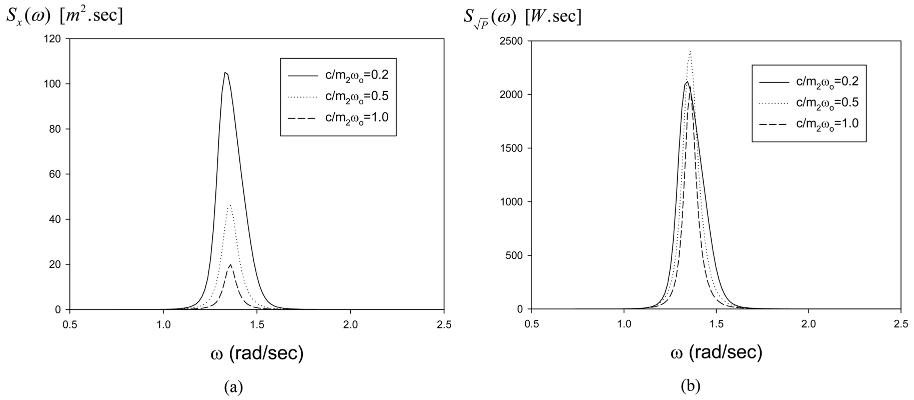


Fig. 15. (a) Relative motion spectrum and (b) square root power spectrum as a function of non-dimensional LEG system damping and wave frequency for $H_{1/3}$ = 2.0 $m$, $\omega_P$ = 1.39red/sec, $k/m_2\omega_o^2$ = 1.0

Table 1. Significant heave amplitude and significant square root power amplitude ($\sqrt{P}_{1/3}$) for $H_{1/3}$ = 2.0 $m$, $\omega_P$ = 1.39 red/sec. $c/m_2\omega_o$ = 0.5

| $\frac{k}{m_2\omega_o^2}$ | $z_{o1/3}$ (m) | $x_{o1/3}$ (m) | $\sqrt{P}_{1/3}$ ($W^{1/2}$) |
|---|---|---|---|
| 0.2 | 3.11 | 3.30 | 23.93 |
| 1.0 | 2.50 | 4.70 | 33.92 |
| 2.0 | 3.26 | 2.61 | 18.88 |

Table 2. Significant heave amplitude and significant square root power amplitude ($\sqrt{P}_{1/3}$) for $H_{1/3}$ = 2.0 $m$, $\omega_P$ = 1.39 red/sec. $k/m_2\omega_o^2$ = 1.0

| $\frac{c}{m_2\omega_o}$ | $z_{o1/3}$ (m) | $x_{o1/3}$ (m) | $\sqrt{P}_{1/3}$ ($W^{1/2}$) |
|---|---|---|---|
| 0.2 | 2.03 | 8.27 | 37.85 |
| 0.5 | 2.50 | 4.70 | 33.92 |
| 1.0 | 2.89 | 2.78 | 28.35 |

relative motion and maximum power-take-off occur at the optimal-spring condition. This can further be confirmed in Table 1. Fig. 15 present similar cases for various damping parameters and fixed spring parameter at its optimal value. As expected, it is seen that we have the maximum relative motion with the minimal damping. However, this is not necessarily so in case of power since the power is proportional to the damping of PTO system. Although we have the maximum amplitude of power at the optimal condition, the band-width of high performance region is greater with $c/m_2\omega_o = 0.2$. Therefore, both amplitudes and band-width of generated power should be considered to achieve maximum efficiency for the given irregular-wave spectrum. This can be confirmed in Table 2, in which we have more power at non-optimal damping value $c/m_2\omega_o = 0.2$ . Finally, in Table 3, the ratio of buoy-heave-resonance frequency and incident-wave spectral peak frequency is

Table 3. Significant heave amplitude and significant square root power amplitude ($\sqrt{P}_{1/3}$) for $H_{1/3}$ = 2.0 $m$, $\omega_P$ = 1.39 red/sec. $c/m_2\omega_o$ = 0.5, $k/m_2\omega_o^2$ = 1.0

| $\omega_o/\omega_P$ | $d$ (m) | $z_{o1/3}$ (m) | $x_{o1/3}$ (m) | $\sqrt{P}_{1/3}$ ($W^{1/2}$) |
|---|---|---|---|---|
| 0.9 | 6.27 | 1.58 | 3.03 | 21.27 |
| 1.0 | 5.00 | 2.45 | 4.62 | 33.24 |
| 1.1 | 4.19 | 2.68 | 4.78 | 35.12 |
| 1.2 | 3.52 | 2.30 | 3.81 | 28.59 |

varied from 0.9 to 1.3. Interestingly, it is seen that we have the maximum power when its ratio is 1.1 instead of 1.0. It is due to the fact that the incident-wave velocity spectrum, $\omega^2 S_\varsigma(\omega)$, has more skew toward higher frequencies, as can be seen in Fig. 13, and the power is proportional to wave velocity instead of wave amplitude. This fact has to be considered in the actual design of the WEC.

## 4. Conclusions

A PTO (power-take-off) mechanism through inner dynamic system inside a floating buoy is suggested. The power take-off system is characterized by mass, stiffness, and damping and generates power through the relative heave motion between the buoy and inner mass. A systematic hydrodynamic theory is developed for the suggested WEC and the developed theory is illustrated by a case study, for which a cylindrical buoy is adopted. The buoy hydrodynamics is solved by the matched eigenfunction expansion method and the buoy-motion results are verified through comparison with the corresponding experiments.

Through the case study, it is seen that the maximum power can be obtained at the optimal condition of spring and damper, as predicted by the developed WEC theory. However, the band-width of high performance region is not necessarily the greatest at the optimal (maximum-power-take-off) condition, so it has to be taken into consideration in the actual design of the WEC for irregular waves. It is desirable to locate the buoy heave-resonance frequency at the frequency about 10% higher than the peak of incident wave spectrum. Whether the high-performance region can further be increased by slightly modifying the buoy particulars or shapes will be the subject of next study.

## Acknowledgments

This work was supported by the New and Renewable Energy of the Korea Institute of Energy Technology Evaluation and Planning(KETEP) grant funded by the Korea government Ministry of Knowledge Economy.(2010302007 0080).

## References

Beatty, S.J., Buckham, B.J. and Wild, P. (2008), "Frequency response tuning for a two body heaving wave energy converter", *Proceedings of the 18th Intl. Conf. Offshore and Polar Eng. (ISOPE)*, Vancouver.

Bouws, F., Gunther, H., Rosenthal, W. and Vincent, C.L. (1985), “Similarity of the wind wave spectrum in finite depth water: 1. spectral form”, *J. Geophys. Res*., **90**(1), 975-986.

Budal, K. and Falnes, J. (1975), “A resonant point absorber of ocean wave power”, *Nature*, **256**, 478-479.

Elwood, D., Rhinefrank. K., Prudell, J., Schacher, A., Hogan, P., Vander Meulen, A., von Jouanne, A., Brekken, T., Yokochi. A. and Yim, S.C. (2007), “Experimental and numerical modeling of direct-drive wave energy extraction devices”, *Proceedings of the Offshore Mechanics and Arctic Engineering Conference*, San Diego, CA, Paper No.OMAE2007- 29728.

Evans, D.V. (1976), “A theory for wave-power absorption by oscillating bodies”, *J. Fluid Mech*., **77**(1), 1-25.

French, M.J. and Bracewell, R.H. (1985), “Heaving point absorbers reacting against an internal mass”, *Proceedings of the IUTAM Int. Symp. on Hydrodynamics of Ocean Wave Energy Utilisation*, Lisbon, Portugal.

Garrett, C.J.R. (1971), “Wave forces on a circular dock”, *J. Fluid Mech*., **46**(1), 129-139.

Gato, L.M.C. and Falcão, A.F.de O. (1988), “Aerodynamics of the wells turbine”, *Int. J. Mech. Sci*., **30**(6), 383-395.

Goda, Y. (1988), “Statistical variability of sea state parameters as a function of a wave spectrum”, *Coastal Eng*. in Japan, **31**, 39-52.

Grilli, A.R., Merrill, J., Grilli, S.T., Spaulding, M.L. and Cheung, J. (2007), “Experimental and numerical study of spar buoy-magnet/spring oscillators used as wave energy absorbers”, *Proceedings of the 17th Intl. Conf. Offshore and Polar Eng*., No.2007-JSC-569.

Kim, M.H. and Choi, H.S. (1983), “Hydrodynamic characteristics of two-dimensional wave energy absorbers”, *J. Soc.Naval Architects of Korea*, **20**(1).

Koo, W.C. and Kim, M.H. (2010), “A nonlinear time-domain simulation of a land-based oscillating water column (OWC)”, *J. Waterway, Port, Coastal Ocean Eng.- ASCE*, **136**, 276-285.

McCormick, M.E. (2007). *Ocean wave energy conversion*, Dover Publication.

McIver, P. and Evans, D.V. (1984), “The occurrence of negative added mass in free-surface problems involving submerged oscillating bodies”, *J. Eng. Math*., **18**(1), 7-22.

Miles, J.W. and Gilbert, F. (1968), “Scattering of gravity waves by a circular dock”, *J. Fluid Mech*., **34**(4), 783-793.

Newman, J.N. (1975), “Interaction of waves with two dimensional obstacles: a relation between the radiation and scattering problems”, *J. Fluid Mech*., **71**(2), 273-282.

Omholt, T. (1978), "A wave activated electric generator", *Proceedings of the "Ocean 78" Marine Technology Conference*, Washington, D.C.

Rho, J.B., Choi, H.S., Park, I.K. and Shin, H.S. (2002), “A Study on the effect of damping devices on motions of SPAR platform”, *Proceedings of the Annual Spring Meeting of the Society of Naval Architects of Korea*.

Srokosz, M.A. and Evans, D.V. (1979), “A theory for wave power absorption by two independently oscillating bodies”, *J. Fluid Mech*., **90**(2), 337-362.

Tung, C.C. (1979), “Hydrodynamic forces on submerged vertical circular cylindrical tanks underground excitation”, *Appl. Ocean Res*., **1**, 75-78.